

論 文 題 目

EphA7<sup>+</sup> perivascular cells as myogenic and angiogenic precursors  
improving skeletal muscle regeneration  
in a muscular dystrophy mouse model.

(EphA7 陽性周細胞は、筋ジストロフィーマウスモデルにおいて、  
骨格筋再生能を改善する)

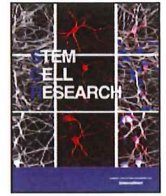
専攻名

旭川医科大学大学院医学系研究科博士課程研究者専攻

著者名

鹿 野 耕 平

(堀内 至、吉田 有里、早坂 太希、鹿原 真樹、富田 唯、竜川 貴光、松尾 梨沙、  
澤田 潤、中川 直樹、竹原 有史、長谷部 直幸、川辺 淳一)



# EphA7<sup>+</sup> perivascular cells as myogenic and angiogenic precursors improving skeletal muscle regeneration in a muscular dystrophic mouse model

Kohei Kano<sup>a,c</sup>, Kiwamu Horiuchi<sup>a,c</sup>, Yuri Yoshida<sup>b,d</sup>, Taiki Hayasaka<sup>a,c</sup>, Maki Kabara<sup>a</sup>, Yui Tomita<sup>b,e</sup>, Takamitsu Tatsukawa<sup>b,d</sup>, Risa Matsuo<sup>b,f</sup>, Jun Sawada<sup>c</sup>, Naoki Nakagawa<sup>c</sup>, Naofumi Takehara<sup>c</sup>, Naoyuki Hasebe<sup>a,c</sup>, Jun-ichi Kawabe<sup>a,b,\*</sup>

<sup>a</sup> Department of Cardiovascular Regeneration and Innovation, Asahikawa Medical University, Asahikawa, 2-1-1 Midorigaoka-higashi, Asahikawa 078-8510, Japan

<sup>b</sup> Department of Biochemistry, Asahikawa Medical University, Asahikawa, 2-1-1 Midorigaoka-higashi, Asahikawa 078-8510, Japan

<sup>c</sup> Department of Medicine, Division of Cardiovascular, Respiratory and Neurology, Asahikawa Medical University, Asahikawa, 2-1-1 Midorigaoka-higashi, Asahikawa 078-8510, Japan

<sup>d</sup> Department of Vascular Surgery, Asahikawa Medical University, Asahikawa, 2-1-1 Midorigaoka-higashi, Asahikawa 078-8510, Japan

<sup>e</sup> Department of Radiology, Asahikawa Medical University, Asahikawa, 2-1-1 Midorigaoka-higashi, Asahikawa 078-8510, Japan

<sup>f</sup> Department of Dermatology, Asahikawa Medical University, Asahikawa, 2-1-1 Midorigaoka-higashi, Asahikawa 078-8510, Japan

## ARTICLE INFO

### Keywords:

Skeletal muscle  
Myogenesis  
Muscular dystrophy  
Pericytes  
Capillary  
Stem cells

## ABSTRACT

Skeletal muscle has a capacity for muscular regeneration mediated by satellite cells (SCs) and non-SCs. Although it is proposed that non-SCs are attractive therapeutic targets for dystrophies, the biological properties of these cells remain unclear. We have recently identified novel multipotent pericytes (PCs), capillary stem cells (CapSCs) derived from the microvasculature. In the present study, we determined if CapSCs contributed to myogenic regeneration using muscular dystrophy mouse model.

CapSCs were isolated as EphA7<sup>+</sup>NG2<sup>+</sup>PCs from the subcutaneous adipose tissues of GFP-transgenic mice. Co-culture with C2C12 myoblast cells showed that CapSCs effectively enhanced myogenesis as compared to controls including EphA7<sup>-</sup>PCs and adipose stromal cells (ASCs). CapSCs transplanted in cardiotoxin-injured gastrocnemius muscles were well differentiated into both muscle fibers and microvessels, as compared to controls. At three weeks after cell-transplantation into the limbs of the *mdx/utrn*<sup>-/-</sup> mouse, CapSCs increased the number of GFP<sup>+</sup> myofibers along with dystrophin expression and the area size of myofibers, and also enhanced the muscular mass and its performance, assessed by treadmill test as compared to controls.

In conclusion, CapSCs have potent myogenic regeneration capacity and improved the pathological condition in a muscular dystrophy mouse. Thus, CapSCs are an attractive cellular source in regenerative therapy for muscular dystrophy.

## 1. Introduction

Duchenne muscular dystrophy (DMD) is the most common and severe inheritable muscle dystrophy in humans (Bushby et al., 2010). DMD is caused by mutations in the gene encoding dystrophin, which lead to dystrophin deficiency at the myofiber membrane and the fragility of the sarcolemma. In response to the continuous muscle fiber degeneration, remarkable potent muscular regeneration mediated by innate myogenic stem cells is repetitively induced. Although muscle regeneration initially supports the mutation-driven muscular degeneration, such regeneration is eventually attenuated due to stem cell

exhaustion (Shi and Garry, 2006).

Satellite cells (SCs) are well-known primary muscle-resident myogenic cells involved in muscle growth and regeneration (Yin et al., 2013). In addition to SCs, there has been evidence that various non-SCs myogenic precursors such as fibro/adipogenic progenitors (Joe et al., 2010), PW1<sup>+</sup>Pax7<sup>-</sup> cells (Mitchell et al., 2010), mesenchymal stem cells (MSCs) also participate in the muscle regenerative process. These data imply the concept that the regenerative potential of skeletal muscle is maintained by the heterogenous population of muscle-resident stem/progenitor cells (Klimczak et al., 2018; Yin et al., 2013). MSCs, which have been identified for a long time, have been considered

\* Corresponding author at: Department of Biochemistry, Asahikawa Medical University, Asahikawa, 2-1-1 Midorigaoka-higashi, Asahikawa 078-8510, Japan.  
E-mail address: [kawabeju@asahikawa-med.ac.jp](mailto:kawabeju@asahikawa-med.ac.jp) (J.-i. Kawabe).

<https://doi.org/10.1016/j.scr.2020.101914>

Received 27 January 2020; Received in revised form 29 June 2020; Accepted 9 July 2020

Available online 21 July 2020

1873-5061/© 2020 The Author(s). Published by Elsevier B.V. This is an open access article under the CC BY license (<http://creativecommons.org/licenses/by/4.0/>).



as the most common cell source for cell-based musculoskeletal regeneration therapies (Klimczak et al., 2018; Phinney and Prockop, 2007). However, current sources of MSCs, consisting of heterogenic cellular populations, provide relatively low frequency of progenitors and limit their therapeutic effects. To overcome these limitations, pericytes (PCs) have been considered as an alternative source of myogenic progenitors (Birbrair and Delbono, 2015; Cathery et al., 2018; Crisan et al., 2008).

Mesoangioblasts (MABs) are vessel-associated stem cells originally isolated from the embryonic dorsal aorta. They have angiogenic and myogenic potency (Minasi et al., 2002). Multipotent cells have been isolated from bone marrow, aorta, and skeletal muscle of postnatal animals with a morphology similar to MABs, which express PC-specific markers such as PDGFR $\beta$ , NG2 (Berry et al., 2007; Corselli et al., 2010; Crisan et al., 2008; Dellavalle et al., 2007). These cells are referred to as multipotent PCs, and defined as PCs expressing CD146, alkaline phosphatase (ALP), but not CD34, CD45 and CD56. PCs have several developmental origins and consist of heterogenous populations (Armulik et al., 2011; Diaz-Flores et al., 2009). However, none of these molecular markers are specific to multipotent PCs (Armulik et al., 2011).

Recent studies using mouse line having reporter and lineage tracing genes driven by marker-promoters have determined specific markers for multipotent PCs. Birbrair et al. reported that nestin<sup>+</sup> PCs are specific to a multipotent PC subtype with restricted lineage myogenic potential, and retains attributes for all PCs independent of their tissue localization (Birbrair et al., 2014a; Birbrair et al., 2013; Birbrair et al., 2014b). Gli1-positive perivascular cells possess MSC-like potency and contribute to organ fibrosis (Kramann et al., 2015; Zhao et al., 2014). As nestin, desmin and transcriptional factors, such as Gli1, are found in the intracellular compartment, it is difficult to utilize them as markers for isolating living cells from human or animal tissues.

Recently, we identified novel multipotent PCs, namely capillary stem cells (CapSCs) with microvessel formation by themselves and mesenchymal and neurogenic potentials (Tomita et al., 2019; Yoshida et al., 2020). CapSCs can be successfully isolated from microvessels-associated cells of peripheral tissues using the specific marker, EphA7 (Yoshida et al., 2020). In this study, we examined the myogenic potency of CapSCs and the effects of their transplantation on the muscular condition of a muscular dystrophy mouse model. CapSCs have myogenic potential; CapSCs that were transplanted into chemically-mediated injured muscles or muscles of a severe muscular dystrophy mouse improved muscle regeneration and muscular performance through their myogenic effects and intramuscular microvascular formation. These findings indicate that CapSCs may function as a potential therapeutic cellular source for muscular dystrophy.

## 2. Material and methods

### 2.1. Preparation of experimental animals

Male C57BL/6 and transgenic mice including actin-promoter-derived GFP(GFP) mice aged 10–12 weeks were used for preparation of GFP-expressing cells (Yamauchi et al., 2013) (Yoshida et al., 2020). The severe muscular dystrophy mouse model (C57BL10-background dystrophin-utrophin double-knockout male homozygous (*dystrophin*<sup>-/-</sup> (*mdx*), *utrophin*<sup>-/-</sup> (*utrn*)) was prepared by crossing those heterozygous mice (Deconinck et al., 1997). Those double male mice were used from 4 to 5 weeks of age. All experiments involving animal studies were performed according to protocols approved by the Animal Care and Use Committee of Asahikawa Medical University. Animals were maintained in a temperature- and light-controlled facility and were fed normal chow.

### 2.2. Preparation of capillary-associated cells and adipose stromal cells (ASCs)

Microvessel fragments were obtained from the subcutaneous adipose tissues. The NG2<sup>+</sup> cells (PCs) were separated from the cells that grew out from microvessel fragments, and EphA7<sup>+</sup> cells and EphA7<sup>-</sup> cells (control PCs, ctPCs) were isolated from prepared PCs by FACS using an anti-EphA7 antibody (LSBio, LS-C3329513, Seattle, WA) as previously described (Yoshida et al., 2020). The subcutaneous adipose tissues were digested with collagenase buffer, then adipose stromal cells (ASCs) were prepared as described previously (Minoshima et al., 2018).

### 2.3. Myogenic differentiation assay

Mouse C2C12 skeletal muscle myoblasts (ATCC) were cultured in complete medium (Dulbecco's modified eagle's medium (DMEM; Gibco Thermo Fisher Scientific, Waltham, MO) containing 1.0 g/L glucose, supplemented with 10% fetal bovine serum (FBS; CORNING, Corning, NY), 100 U/mL penicillin and 100  $\mu$ g/mL streptomycin). Cells were seeded onto collagen-coated eight chamber slides (IWAKI, Shizuoka, Japan). When cell culture reached 70–90% confluency, the medium was switched to differentiation medium (DMEM containing 2% horse serum (Gibco Thermo Fisher Scientific, Waltham, MO), 100 U/mL penicillin and 100  $\mu$ g/mL streptomycin) which enhances myoblast fusion (Dellavalle et al., 2007). The medium was exchanged every 4 days and myogenic differentiation was confirmed by observation of myotube formation or immunostaining of myosin heavy chain (MHC). For each data, the mean of ratio of MHC-immunostaining area to total observation area in three pictures (40 $\times$ ) was measured.

### 2.4. Muscle injury model

To induce muscle damage, 100  $\mu$ L of 150  $\mu$ M cardiotoxin (CTX; Sigma-Aldrich) was injected intramuscularly into the gastrocnemius of anesthetized mice. After 24 h of CTX-mediated muscle damage, GFP-expressing cells ( $1.0 \times 10^6$  cells in 100  $\mu$ L PBS) were injected intramuscularly into the damaged muscles. At 3 weeks after transplantation, the mice were euthanized, and the muscles were immediately harvested and used for histological analyses or were flash frozen in liquid nitrogen and stored at  $-80^\circ\text{C}$  until molecular analyses.

### 2.5. Exercise tolerance tests

Mice were subjected to an exhaustion treadmill test by placing them on the belt of a one-lane motorized treadmill (TMS-4B Treadmill for Mice; MELQUEST, Toyama, Japan) (Dellavalle et al., 2007). The test was started at an inline of 0 at 10 m/min for 10 min; thereafter, the speed was increased by 1 m/min every minute. After 10 min, the treadmill was stopped and mice rested for 5 min. After the 5-minute resting period, the exercise was restarted at 10 m/min for 60 min. When mice were not able to sustain running or run the whole distance (600 m), the treadmill was stopped, and the running distance was measured.

### 2.6. Ultrasonographic analysis

Mice were anesthetized with 2% isoflurane and their hindlimbs were shaved. Holding ultrasonic probe to the gastrocnemius, images of the long axis muscle were obtained (Vevo 2100; VisualSonics, Toronto, Canada). The gastrocnemius margin was traced, and muscle area was measured using the Vevo 2100 software.

### 2.7. Immunofluorescence analysis

Immunohistochemical and immunofluorescence analyses were conducted as described in previous reports (Kabara et al., 2014;



**Table 1**  
Gene expression array profile I (cellular markers) of primary CapSCs and ctPCs.

Marker	Gene			Gene expression			References
	MGI ID	symbol	discription	ctPCs	CapSCs	log2(ratio)	
Pericyte (PC)	97,531	PDGFR $\beta$	platelet derived growth factor receptor, beta	1356	601	-1.17	# (Armulik et al., 2011)
	2,153,093	NG2(Cspg4)	chondroitin sulfate proteoglycan 4	292	168	-0.80	# (Armulik et al., 2011)
	1,933,966	CD146	melanoma cell adhesion molecule	265	202	-0.39	# (Crisan et al., 2008)
	76,365	Tbx18	T-box18	23	25	0.10	(Guimaraes-Camboa et al., 2017)
Multipotent PC	11,647	Akp2	alkaline phosphatase2	24	12	-1.00	(Dellavalle et al., 2007)
	101,784	nestin	nestin	67	247	1.88	# (Birbrair et al., 2013)
	13,346	Des	desmin	11	7	-0.76	(Goritz et al., 2011)
	14,632	Gli1	GLI-Kruppel family member GLI1	18	16	-0.12	(Zhao et al., 2014)
	18,616	PW1 (Peg3)	paternally expressed 3	11	26	1.01	(Mitchell et al., 2010)
CapSC	95,276	Epha7	Eph receptor A7	10	114	3.50	# (Yoshida et al., 2020)
Satellite Cells	17,928	Myog	myogenin	4	6	0.58	
	17,927	MyoD	myogenicdifferentiation1	41	29	-0.50	
	17,877	Myf5	myogenic factor 5	4	7	0.81	
	18,505	Pax3	paired box gene 3	4	5	0.31	
	18,509	Pax7	paired box gene 7	3	5	0.74	

Microarray gene expression comparison between CapSCs and ctPCs (three-independent isolated sample). The detected signal for each gene was normalized with the global normalization method and averaged across triplicates. For a gene expression to be considered significant, it had to have an average fluorescence value above 100 (shaded). #; values are also demonstrated in previous paper (Yoshida et al., 2020).

Minoshima et al., 2018; Tomita et al., 2019). Hematoxylin-eosin staining was conducted on paraffin sections using standard methods. Immunofluorescence was carried out on 10- $\mu$ m-thick frozen gastrocnemius sections and myofibres. The frozen sections and myofibres were fixed with 4% paraformaldehyde (PFA) for 20 min and incubated with 0.3% Triton X-100 in PBS (PBST) for 30 min at room temperature, washed and then incubated with blocking buffer (1%BSA in PBST). Primary antibodies: anti-GFP (ab6673, 1:100: Abcam, Camb, UK), anti-dystrophin (ab15277, 1:100: Abcam), and anti-myosin heavy chain (ab91506, 1:100: Abcam) were used and, bound antibodies were visualized with a secondary antibody conjugated to Alexa 488, Alexa 594 or Alexa647 (Life Technologies, CA, USA). Nuclei were stained with Hoechst 33,342 (H3570, Life Technologies). Images were recorded using a fluorescence microscope (BZ-X710; Keyence, Osaka, Japan). In order to observe the transplanted cells within skeletal muscle tissues in three-dimensions, we made PFA-fixed tissues transparent using a CUBIC reagent (Susaki et al., 2014). Clarified muscular samples were imaged using a confocal fluorescence microscope (FV1000D Olympus) and 20 serial slides in 15  $\mu$ m steps were z-stacked and projected (Tomita et al., 2019). The myotube area, GFP positive myofibres area, and dystrophin positive myofiber areas were measured using the BZ-X Analyzer software (Keyence) and Photoshop (Adobe Systems Incorporated, SJC, USA).

## 2.8. Quantitative reverse-transcription (RT) PCR analyses

Total RNA was isolated from skeletal muscle tissues using the Trizol LS reagent (Invitrogen, California, USA). For quantitative PCR analysis, extracted RNA was reverse-transcribed using iScript Reverse Transcription Supermix for RT-qPCR (Bio Rad; Hercules, California, USA), according to the manufacturer's instructions. The synthesized cDNA was amplified with real-time PCR on a 7300 PCR system (Applied Biosystems; Foster City, CA) using mouse-specific primers and probes. Real-time PCR was carried out using the TaqMan Gene Expression Master Mix (Applied Biosystems) according to the manufacturer's instructions. Absolute threshold values (Ct values) were determined with SDS software 2.1 (Applied Biosystems). Fold changes in target gene expression were calculated via the formula,  $\Delta$ Ct = Ct target-CT control and were normalized to GAPDH expression via the published comparative  $2^{-\Delta$ Ct}.

## 2.9. Gene expression profiling and data analyses

Total cellular RNA was isolated from sorted CapSCs and ctPCs (three independent isolated cell sample), and used for microarray analysis on a 3D-Gene Mouse Oligo Chip 24 K (Toray Industries Inc., Tokyo, Japan) as described previously (Yoshida et al., 2020). Value intensities greater than two standard deviations (SD) above the background signal intensity were considered significant. The detected signal for each gene was normalized by the global normalization method and averaged across triplicates. For a gene to be considered expressed, it had to have an average fluorescence value above 100 (arbitrarily set).

## 2.10. Statistical analysis

Experimental data are presented as mean  $\pm$  SEM unless otherwise noted. Sample number (n) is shown in the figure legends. The statistical significance of differences was evaluated using one-way ANOVA. Nonparametric data (i.e. muscle weight, ultrasonographic muscle area, GFP positive myofiber area, GFP gene expression, running distance) were assessed by the Mann-Whitney U test.  $p < 0.05$  was considered to be statistically significant.

## 3. Results

### 3.1. In vitro myogenic differentiation potency of CapSCs

CapSCs (EphA7<sup>+</sup>PCs) and EphA7<sup>-</sup>ctPCs were isolated from NG2<sup>+</sup>PCs derived from the mouse subcutaneous adipose tissues as described previously (Yoshida et al., 2020). CapSCs have multipotency to differentiate into mesenchymal cells and vascular cells including endothelial cells (ECs) and PCs, whereas ctPCs have no multipotency. Microarray analysis demonstrated that both CapSCs and ctPCs equally expressed PC-specific genes such as PDGFR $\beta$ , NG2, Tbx18 and CD146 (Armulik et al., 2011; Guimaraes-Camboa et al., 2017) (Table 1). Typical gene markers for skeletal muscle progenitor/satellite cells (SCs) were low or no expression in both CapSCs and ctPCs (Table 1). Recently, several markers have been proposed for detection and prospective isolation of multipotent PCs from various kinds of tissues (Birbrair et al., 2014b; Goritz et al., 2011; Mitchell et al., 2010; Zhao et al., 2014). Nestin was selectively expressed in CapSCs compared to ctPCs (Table 1). However, the other marker genes such as desmin, Gli1 and PW1 was less expressed in both CapSCs and ctPCs.

The myoblast cell line, C2C12, can differentiate into myosin-heavy



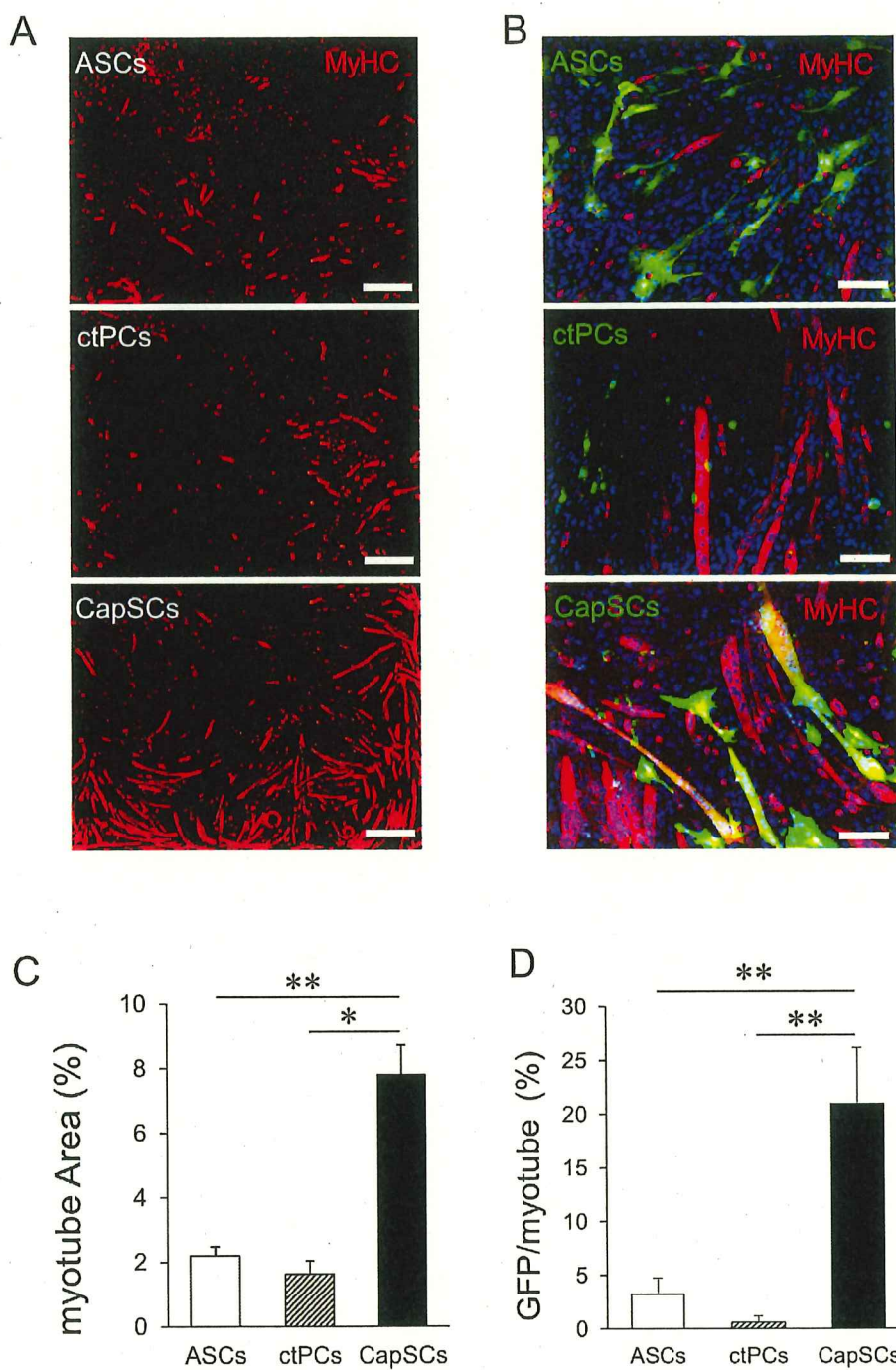


**Fig. 1.** Myogenic potency of CapSCs. C2C12 cells, myoblast cells were co-cultured with GFP-expressing EphA7<sup>+</sup>PC (CapSCs), EphA7<sup>-</sup> control PCs (ctPCs) and ASCs. Differentiated myotubes were determined by immunostaining of the myosin heavy chain (MyHC) (red), and localization of GFP-expressing cells (green) were determined by immunostaining (A, B). Scale bars = 300  $\mu$ m (A), 100  $\mu$ m (B). (C) Formation of myotubes was determined as the ratio of the MyHC-stained area to the total observed area. (D) GFP-positive myotubes were determined as the ratio of the GFP/MyHC-double stained area to the total MyHC-stained area. Data are represented as the means  $\pm$  SEM. \* $p$  < 0.05, \*\* $p$  < 0.01 ( $n$  = 14). (For interpretation of the references to colour in this figure legend, the reader is referred to the web version of this article.)

chain (MyHC)-positive myotubes under myogenic differentiation culture conditions. CapSCs and other control cells alone did not form MyHC-stained myotubes under this culture condition (*data not shown*). However, when CapSCs, but not ASCs or ctPCs, were co-incubated with C2C12, the formation of MyHC-stained myotubes was significantly increased (Fig. 1A, C). GFP-expressing cells were used to observe the localization of the co-incubated cells in myotube formation. GFP-stained myotubes were well observed in the CapSC group but rarely in the ASC or ctPC groups (Fig. 1B, D).

### 3.2. CapSCs differentiated into muscle fibers and microvessels in injured skeletal muscles.

To examine if CapSCs had myogenic potency *in vivo*, cells were transplanted into the gastrocnemius muscle that was damaged by

cardiotoxin (CTX). Upon muscular damage, regenerated muscle fibers, of which nuclei were located at the center of myofibers, were observed by their innate regeneration potency without any fibrotic or fatty degeneration, and attenuated muscle mass was gradually recovered within 1–2 months. In the CapSC-transplanted group, regenerated muscle fibers were observed at three weeks without fibrotic and fatty degeneration (Fig. 2A). Transplanted exogenous GFP-expressing cells were identified with a fluorescence signal in the muscle tissue; specificity was confirmed using an appropriate negative control, *i.e.* non-transplanted tissue. Furthermore, GFP-expression was also confirmed by immunostaining using anti-GFP antibody after quenching endogenous fluorescence using autofluorescence quencher (Fig. 2F).

In CapSC group, GFP-positive myofibers were observed in the regenerated muscle tissues and GFP-signal were also merged with the microvascular endothelium and located at perivascular sites (Fig. 2C, E,



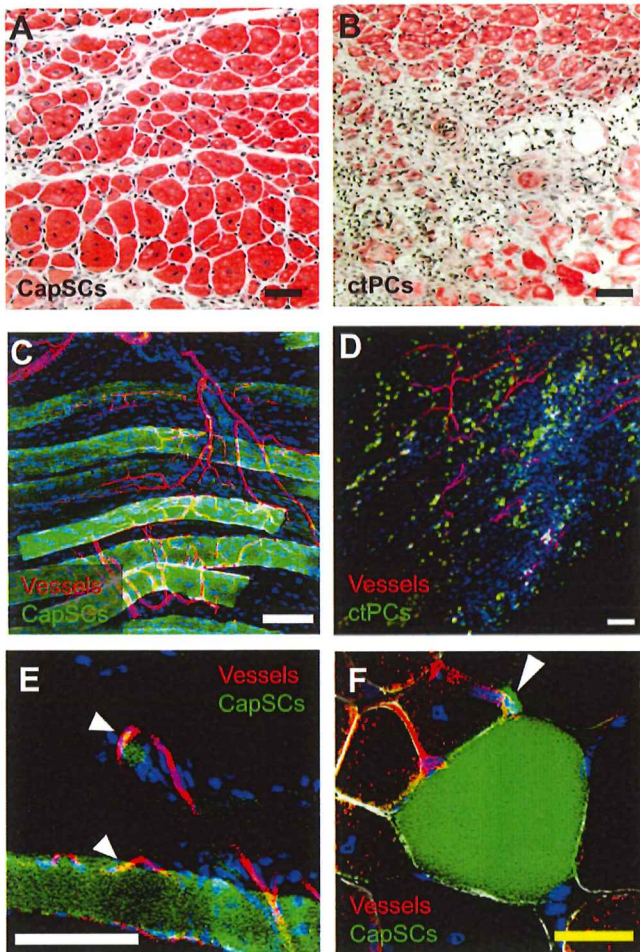


**Fig. 2.** Localization of transplanted CapSCs in injured skeletal muscles. GFP-expressing CapSCs and ctPCs were transplanted into cardiotoxin-injured gastrocnemius muscle. After three weeks of cellular transplantation, hematoxylin-eosin staining (A, B), and immunofluorescence imaging (C-F) were performed. Transplanted cells (green) and lectin-Rhodamine-stained microvessels (red) are shown in a representative 3-dimensional view (C, D) and a single confocal view (E). Immunostaining against GFP was performed after quenching auto-fluorescence and shown in short axis view (F). Arrow head indicates the GFP-signals merged with microvessels. Scale bars = 50  $\mu$ m (A-B), 100  $\mu$ m (C-E), 20  $\mu$ m (F). (For interpretation of the references to colour in this figure legend, the reader is referred to the web version of this article.)

F). Consistent with this finding, we previously reported that CapSCs differentiated to endothelial cells and PCs, and formed microvasculature in the ischemic tissues (Yoshida et al., 2020). In contrast, in the ctPC-transplanted group, fibrotic lesions were observed within damaged muscles (Fig. 2B), and GFP-positive signals were observed within fibrotic lesions, but rarely in regenerated myofibers (Fig. 2D). The number of GFP<sup>+</sup> myofibers in the skeletal muscles was higher in the CapSCs-transplanted group compared to ctPCs group (Supplemental Fig. 1).

### 3.3. CapSCs had potent myogenic regenerative effects for injured skeletal muscle

We further investigated the myogenic effects of CapSCs compared to ASCs, which were previously reported to have myogenic effects (Rodriguez et al., 2005). At three weeks post-CTX-mediated muscular injury followed by transplantation of GFP-expressing cells, GFP<sup>+</sup> myofibers were observed in both CapSC and ASC transplanted muscles (Fig. 3A). However, the number of GFP<sup>+</sup> myofibers in the transplanted muscles was significantly higher in the CapSC group compared to the

ASC group (Fig. 3B). We also confirmed that the expression level of the exogenous GFP gene in the transplanted muscles was higher in the CapSC group (Fig. 3C). Consistent with these findings, muscular mass was increased in the CapSC group, but not in the ASC group (Fig. 3D). These data indicated that CapSCs have both superior tissue retention and myogenic capacities within the injured muscles.

### 3.4. CapSCs differentiated into dystrophin-expressing muscle fibers in dystrophic muscles

Finally, we examined the therapeutic effect of CapSCs having potent myogenic effects using a severe muscle dystrophy mouse model. GFP-expressing cells, CapSCs and ASCs were transplanted into limbs intramuscularly in *mdx/utrn*<sup>-/-</sup> mice. After three weeks of normal breeding, central nuclear myofibers were abundantly observed in the dystrophy muscle tissue in three groups, i.e. PBS-, ASCs-, or CapSCs-transplanted groups, and GFP-positive myotubes were well observed in CapSC- and ASC-transplanted muscles (Fig. 4A). However, the number of GFP-positive myotubes in the gastrocnemius muscle area and the efficiency of the tissue retention assessed by the expression level of the exogenous GFP gene were significantly higher in the CapSC group compared to the ASCs group (Fig. 4B, D).

In the dystrophy mouse, intact dystrophin protein was not detected in myotubes due to the genetic abnormality in the *dystrophin* gene (Fig. 4A). In CapSCs and ASCs-treated groups, dystrophin was mostly detected in GFP-positive myotubes (Fig. 4A). With the increase in the number of GFP-positive myotubes, the number of dystrophin-positive myotubes also increased in the CapSC group (Fig. 4C). The histogram of the short axial area of each myotube within the gastrocnemius muscle demonstrated that the size of the myofibers was increased in the CapSC group compared to the non-treated group (PBS), and was significantly greater than that of ASC group (Fig. 4E, F). In addition to the enhanced size of the myofibers, the number of microvessels around each myofiber increased in the CapSC group (Supplemental Fig. 2A, B). Similar to that in CTX-induced muscle damage model (Fig. 2), the transplanted GFP-expressing cells were well co-localized at the lectin-positive microvasculature (Supplemental Fig. 2A, C).

### 3.5. CapSCs improved the pathological condition in a muscular dystrophy mouse

To examine if the potent myogenic effects of CapSCs contributed to physiological improvement of the muscular dystrophy mouse, muscle mass *in vivo* was estimated by ultrasonography (Fig. 5A) and the wet weight of isolated gastrocnemius muscles was determined. CapSCs significantly increased muscle mass and its weight as comparison to PBS, i.e. the non-treated group, and these parameters in the CapSC group were higher compared to that of the ASC group (Fig. 5B, C). In addition to muscle mass, muscular performance as estimated by treadmill analysis was also significantly improved in the CapSC group (Fig. 5D). There was no difference in total body weight among these groups within the observation period (Fig. 5E).

## 4. Discussion

In addition to the satellite cells, several myogenic interstitial and perivascular cell populations have been reported. In the present study, we demonstrated that EphA7<sup>+</sup> PCs (CapSCs) derived from the microvessels of peripheral subcutaneous adipose tissues have myogenic potency in the dystrophic mouse model. To examine the similarity and difference in CapSCs with the previously reported multipotent cells, we compared the expression levels of specific gene markers for these cells between CapSCs and EphA7<sup>-</sup> PCs (ctPCs) (Table 1). Among these marker genes, CapSCs and ctPCs are represented as nestin-expressing and non-nestin-expressing PCs, respectively. Recent study by Birbrair et al. performed on the nestin-GFP expressing transgenic mice,



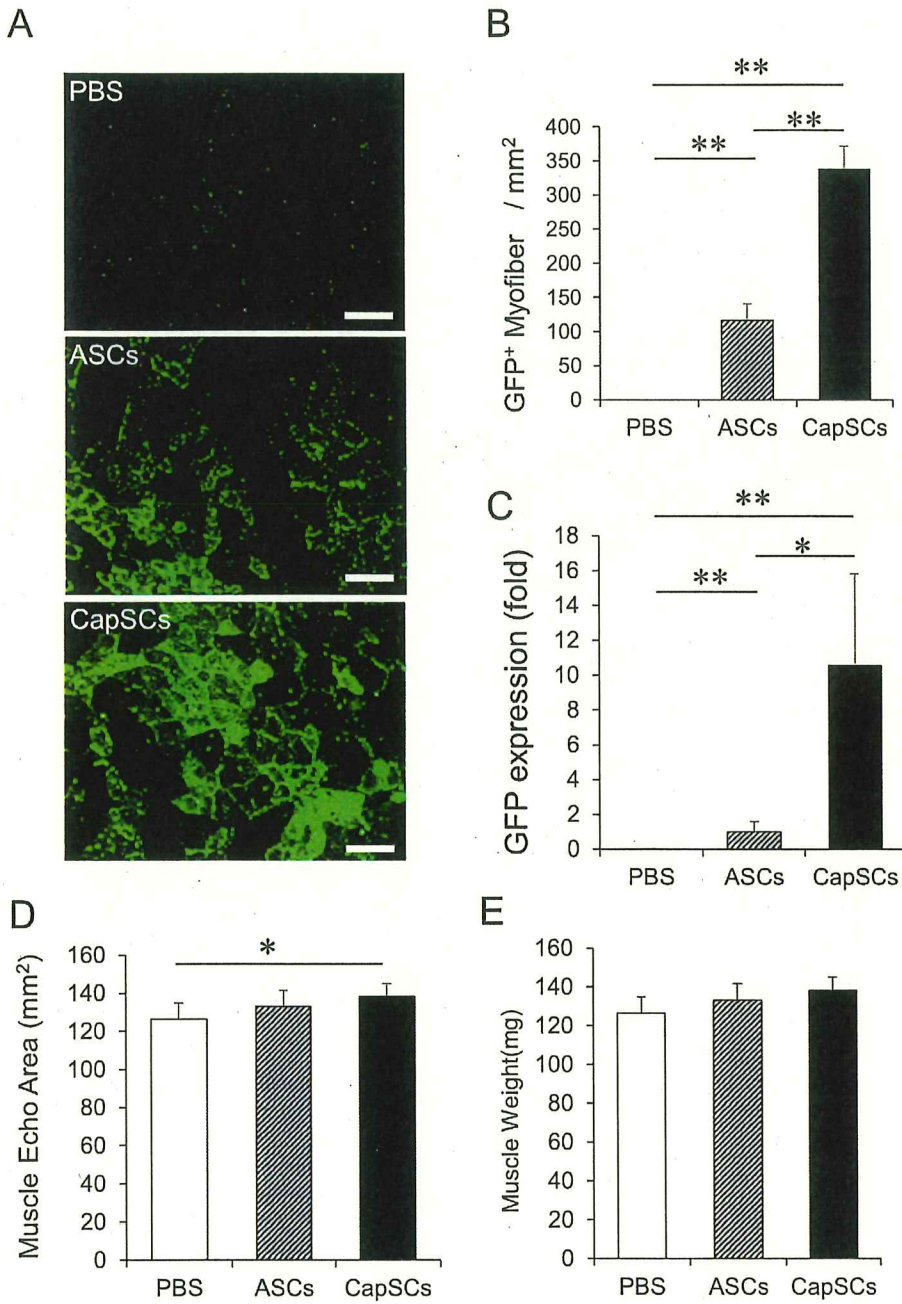


**Fig. 3.** CapSCs are retained in injured skeletal muscles and improved the regeneration of muscle. CapSCs and ASCs or PBS were transplanted into cardiotoxin-injured gastrocnemius muscle. After three weeks of transplantation, transplanted GFP-expressing cells (green) were observed by fluorescence microscopy. (A) Representative short axial view of muscles of each group. Scale bars = 100  $\mu$ m. (B) The GFP-positive myofibers was counted in the gastrocnemius muscle area and expressed the number of GFP + myofibers per area. (C) Expression of mRNA levels of the exogenous *GFP* gene in the transplanted muscles was estimated by qRT-PCR. (D) The long axial area of gastrocnemius muscles *in vivo* was estimated by ultrasonography. Data are represented as the means  $\pm$  SEM. \* $p$  < 0.05, \*\* $p$  < 0.01 (n = 5–7). (For interpretation of the references to colour in this figure legend, the reader is referred to the web version of this article.)

demonstrated that type I and II PCs were identified by nestin expression (Birbrair et al., 2013). Nestin<sup>-</sup> type I PCs have the potential to trans-differentiate into adipogenic and fibrogenic lineage, whereas nestin<sup>+</sup> type II PCs possess myogenic, neurogenic, and angiogenic potential (Birbrair et al., 2014a; Birbrair et al., 2013; Birbrair et al., 2014b). As demonstrated in the present and previous studies, CapSCs have MSC-like multipotency in addition to myogenic, neurogenic, and angiogenic potential (Tomita et al., 2019; Yoshida et al., 2020). In contrast, ctPCs, which are nestin<sup>-</sup> PCs, are not MSC-like cells and have neither adipogenic (Yoshida et al., 2020) nor myogenic potency (Fig. 2B, Supplemental Fig. 1B). These two cell populations (CapSCs/ctPCs and type I/II PCs) show several differences in not only the cellular characteristics, but also the kind of tissue source (adipose tissues and skeletal muscles respectively), and the cellular preparation method. Although it was observed that these multipotent PCs are both highly nestin-expressing cells, it is unclear whether CapSCs are overlap with type II PCs physically in tissues or just in marker gene expression. Nevertheless,

importance of the present study is to identify the specific marker, EphA7, to isolate myogenic potent multipotent PCs from normal tissues, *i.e.* the subcutaneous adipose tissues, which are easy to prepare in the clinical setting. This is substantially advantageous in the clinical application.

Because myonuclei within muscle fibers are postmitotic, regeneration and maintenance of multinuclear myofibers must be mediated by cellular fusion of myoblasts which are differentiated from myogenic progenitors or stem cells (Deng et al., 2017). GFP-positive myofibers were observed after transplantation of GFP-expressing CapSCs and intact dystrophin was expressed in these regenerated myofibers (Fig. 4). The data suggest that CapSCs may differentiate into myoblasts to fuse with preexisting myofibers, resulting in the expression of GFP and myocyte-related intact genes such as dystrophin. *In vitro* coculture with C2C12 indicated that CapSCs effectively stimulated myogenesis, forming myotubes and the fusion to myotubes, although CapSCs alone did not differentiate into myoblast (Fig. 1). Trophic effects by

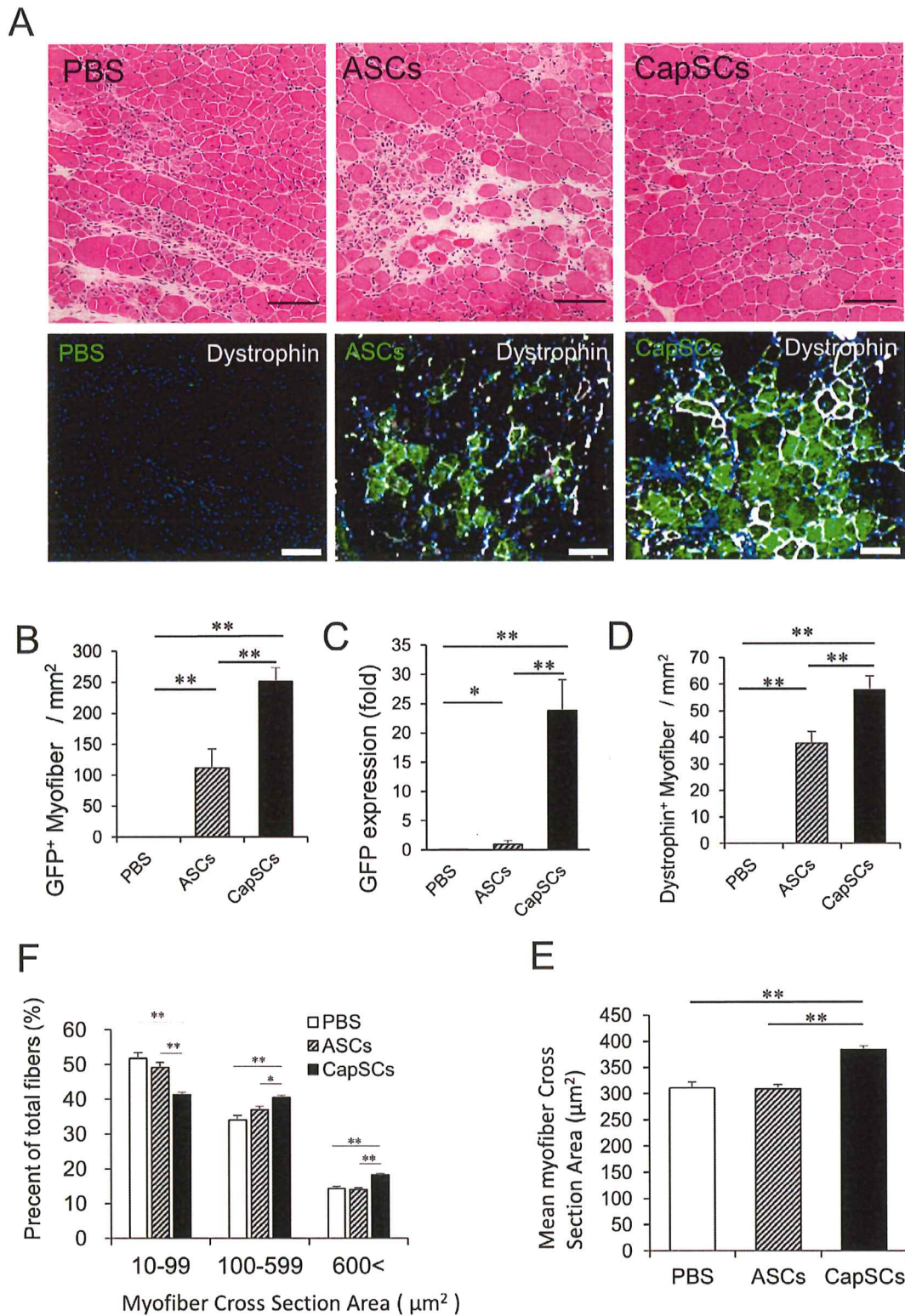


Fig. 4. Localization of transplanted CapSCs in skeletal muscles of an *mdx/utrn*<sup>-/-</sup> muscular dystrophy mouse. (A) After three weeks of normal breeding after transplantation of GFP-expressing cells into limbs muscles of the muscular dystrophy mouse, the tissue slide was stained with hematoxylin-eosin and the GFP-signal (green) and dystrophin (white) were determined by immunostaining. Scale bars = 100 μm. In short axis section of muscles, the numbers of the GFP-positive myofibers (B), and the dystrophin-expressing myofibers (C) were counted in the gastrocnemius muscle area. (D) Expression of mRNA levels of exogenous *GFP* gene in the isolated muscles was estimated by qRT-PCR. In short axial sections of gastrocnemius muscle, the area of each myotube was estimated and demonstrated in the histogram (E), and the area average of total myotubes was calculated (F). Data are depicted as the means ± SEM. \**p* < 0.05, \*\**p* < 0.01 (n = 7–12). (For interpretation of the references to colour in this figure legend, the reader is referred to the web version of this article.)



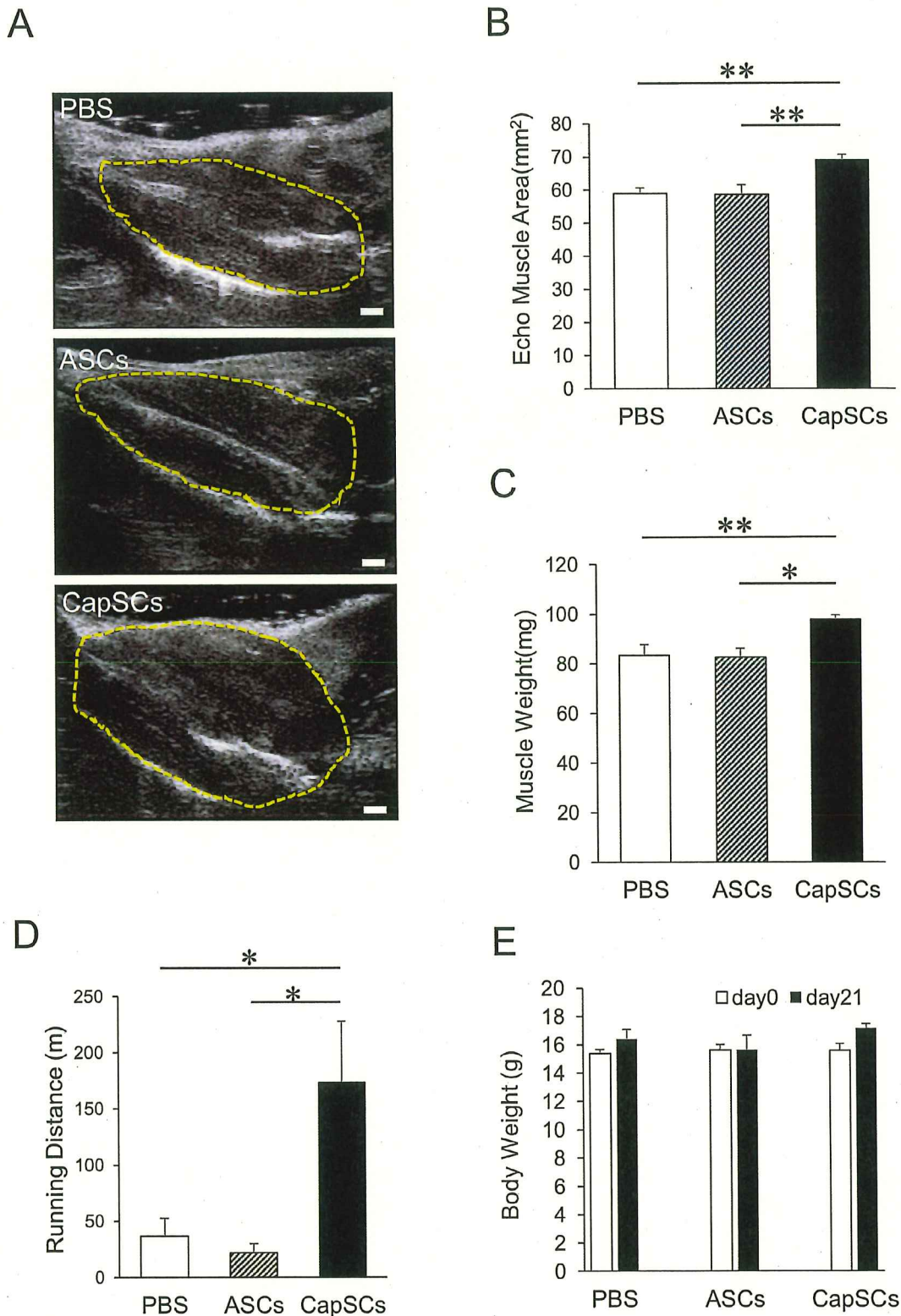


Fig. 5. Effects of CapSC transplantation on muscle mass and performance in a muscular dystrophy mouse. CapSCs, ASCs and PBS were transplanted into gastrocnemius muscle of *mdx/utrn*<sup>-/-</sup> dystrophy mice. After three weeks of transplantation, muscle mass was estimated by ultrasonography (A, B) and the wet weight of isolated gastrocnemius muscle (C). Representative ultrasonographic long axial views of muscles are shown (A), and their traced area was estimated (B). Scale bars = 1 mm. The total running distance of each mouse group are estimated in treadmill exercise tolerance experiments (D). Body weight are also measured before and after cellular transplantation (E). Data are depicted as the means  $\pm$  SEM. \**p* < 0.05, \*\**p* < 0.01 (n = 12).

preexisting myoblasts/myofibers might be required to induce CapSCs to differentiate into myoblasts. Similar to CapSCs, aorta-derived MABs require coculture with skeletal myoblasts for their myogenic potency, in contrast to skeletal muscle-derived MABs, which spontaneously

differentiate into myoblasts (Dellavalle et al., 2007; Diaz-Manera et al., 2010).

In the muscular dystrophy model, chronic and persistent muscle damage reduces self-muscular regeneration potency (Deconinck et al.,



1997). Therefore, in contrast to the CTX-induced muscular injury model (Fig. 3D), supplementation of muscular precursor/stem cells induces effective muscular regeneration in the muscular dystrophy model. CapSCs did not detect in the non-injured skeletal muscles of wild type mice after 21 days of cellular transplantation (*data not shown*). However, CapSCs showed excellent retentivity in the skeletal muscles of muscular dystrophy mice and effective myogenic differentiation potency (Fig. 4). In contrast to human cases of muscle dystrophy, pseudo-hypertrophy such as adipose deposition was not observed in the severe dystrophy mouse model. Transplanted CapSCs were detected in skeletal myotubes along with dystrophin expression and improved the muscular mass and their performance compared to ASCs- and non-treatment groups (Fig. 5). Therefore, the muscle regenerative effect of CapSCs relies on the regeneration of non-fragile myocytes having intact dystrophin.

We had previously reported that CapSCs have potent angiogenic activity, *i.e.* they can differentiate to vascular cells to form microvessels (Yoshida et al., 2020). Transplanted CapSCs were observed at the microvessels in the regenerated muscle tissues (Fig. 2E, F). Therefore, in addition to the direct myogenic effects, the angiogenic effects of CapSCs could contribute to their muscular regeneration potency in a dystrophic mouse model. In this study, the number of capillaries around each myotube and the ratio of transplanted cells colocalized in these capillaries are increased especially in the CapSC-transplanted group (Supplemental Fig. 2). Capillaries act as blood ducts delivering oxygen and nutrients to tissue parenchymal cells and grows according to the demand of oxygen by these cells. Therefore, the increased microvasculature around the myofiber may be primarily due to the enhanced size of the myofibers. However, the significance of the transplanted CapSCs effectively retained at the microvasculature around myofibers remains to be clarified.

For ideal long-term muscle regenerative therapy for inheritable muscle dystrophy, at least two conditions, *i.e.* not only increasing the regeneration of non-fragile myocytes but maintaining the pool of myogenic progenitor/stem cells possessing intact genes within skeletal muscles would be required. It has been reported that the microvasculature is one of specific niches for the maintenance of stem cells (Khan et al., 2016; Mendelson and Frenette, 2014; Morrison and Scadden, 2014). Therefore, microvessels play a role in not only a blood derived duct but also a stem cell reservoir. Multipotent CapSCs are originally located at perivascular sites as mural cells (Tomita et al., 2019; Yoshida et al., 2020). Thus, it is postulated that transplanted CapSCs which are maintained as myogenic stem cells at peri-vascular sites contribute to the self-myogenic regeneration for the remaining life span. It should be investigated whether transplanted CapSCs within microvessels act as progenitors or stem cells for myogenic regeneration during relative long period. The severe dystrophy mouse, *mdx/utrn*<sup>-/-</sup> mouse model has a short life span (approximately 50% mortality within 6-month-old) due to the cardio- and progressive muscular dysfunction (Hayashiji et al., 2015). In the present study, CapSCs were transplanted into *mdx/utrn*<sup>-/-</sup> limbs at 4–5 weeks of age. The muscle mass and performance of limbs muscles where CapSCs were transplanted were significantly improved (Fig. 5) and there was no apparent difference in mortality during one-month observation period (Supplemental Fig. 2C). Further investigations focusing on the life-span, long-term effects of global transplantation of CapSCs, *e.g.* via intravascular injection would be required for understanding the further therapeutic potential of CapSCs for muscular dystrophy.

In conclusion, we demonstrated that novel multipotent PCs, CapSCs have a potent myogenic capacity and improved muscle regeneration and its physiological performance in a severe muscular dystrophy mouse model. CapSCs may function as an attractive therapeutic cellular source for muscular dystrophy.

## Author contributions

K.K.: performed cell biology and animal experiments and analyzed data, data interpretation, manuscript writing. K.H., Y.Y., Y.T. and J.S.: performed cell biology and animal experiments and analyzed data. T.H., and N.T.: assisted with flow cytometric analysis. M.K., T.T., R.M., S.Y. and N.N.: helped with biochemical and histological analysis and discussion. N.H. supervised the research. J.K.: conception and design, data interpretation, manuscript writing, final approval manuscript.

## Declaration of Competing Interest

The authors declare that they have no known competing financial interests or personal relationships that could have appeared to influence the work reported in this paper.

## Acknowledgements

We also thank S. Takahashi, K. Kanno, Y. Horikawa, M. Ishizaka for laboratory assistance; and M. Kusakabe and A. Oda for assistance with FACS experiments. We also thank Dr. N. Ogawa for technology transfer support. This work was supported by JSPS KAKENHI grant number (17H04170, 17K19368 to J. K. and 19K16969 to K.K.) and supported in part by Daiichi Sankyo Co. Ltd., and Asbio Pharmar Co. Ltd. And OideCapiSEA, Inc.

## Competing of interests statement

The authors declare no competing interests.

## Patent pending

PCT/JP2016/072259.

## Appendix A. Supplementary data

Supplementary data to this article can be found online at <https://doi.org/10.1016/j.scr.2020.101914>.

## References

- Armulik, A., Genove, G., Betsholtz, C., 2011. Pericytes: developmental, physiological, and pathological perspectives, problems, and promises. *Dev. Cell* 21, 193–215.
- Berry, S.E., Liu, J., Chaney, E.J., Kaufman, S.J., 2007. Multipotential mesoangioblast stem cell therapy in the *mdx/utrn*<sup>-/-</sup> mouse model for Duchenne muscular dystrophy. *Regen Med* 2, 275–288.
- Birbrair, A., Delbono, O., 2015. Pericytes are essential for skeletal muscle formation. *Stem Cell. Rev. Rep.* 11, 547–548.
- Birbrair, A., Zhang, T., Files, D.C., Mannava, S., Smith, T., Wang, Z.M., Messi, M.L., Mintz, A., Delbono, O., 2014a. Type-1 pericytes accumulate after tissue injury and produce collagen in an organ-dependent manner. *Stem Cell Res. Ther.* 5, 122.
- Birbrair, A., Zhang, T., Wang, Z.M., Messi, M.L., Enikolopov, G.N., Mintz, A., Delbono, O., 2013. Skeletal muscle pericyte subtypes differ in their differentiation potential. *Stem Cell Res.* 10, 67–84.
- Birbrair, A., Zhang, T., Wang, Z.M., Messi, M.L., Olson, J.D., Mintz, A., Delbono, O., 2014b. Type-2 pericytes participate in normal and tumoral angiogenesis. *Am. J. Physiol. Cell Physiol.* 307, C25–C38.
- Bushby, K., Finkel, R., Birnkrant, D.J., Case, L.E., Clemens, P.R., Cripe, L., Kaul, A., Kinnett, K., McDonald, C., Pandya, S., Poysky, J., Shapiro, F., Tomezscko, J., Constantin, C., D.M.D.C.C.W. Group, 2010. Diagnosis and management of Duchenne muscular dystrophy, part 1: diagnosis, and pharmacological and psychosocial management. *Lancet Neurol.* 9, 77–93.
- Catherly, W., Faulkner, A., Maselli, D., Madeddu, P., 2018. Concise review: the regenerative journey of pericytes toward clinical translation. *Stem Cells*.
- Corselli, M., Chen, C.W., Crisan, M., Lazzari, L., Peault, B., 2010. Perivascular ancestors of adult multipotent stem cells. *Arterioscler. Thromb. Vasc. Biol.* 30, 1104–1109.
- Crisan, M., Yap, S., Casteilla, L., Chen, C.W., Corselli, M., Park, T.S., Andriolo, G., Sun, B., Zheng, B., Zhang, L., Norotte, C., Teng, P.N., Traas, J., Schugar, R., Deasy, B.M., Badyrak, S., Buhring, H.J., Giacobino, J.P., Lazzari, L., Huard, J., Peault, B., 2008. A perivascular origin for mesenchymal stem cells in multiple human organs. *Cell Stem Cell* 3, 301–313.
- Deconinck, A.E., Rafael, J.A., Skinner, J.A., Brown, S.C., Potter, A.C., Metzinger, L., Watt, D.J., Dickson, J.G., Tinsley, J.M., Davies, K.E., 1997. Utrophin-dystrophin-deficient



- mic mice as a model for Duchenne muscular dystrophy. *Cell* 90, 717–727.
- Dellavalle, A., Sampaioles, M., Tonlorenzi, R., Tagliafico, E., Sacchetti, B., Perani, L., Innocenzi, A., Galvez, B.G., Messina, G., Morosetti, R., Li, S., Belicchi, M., Peretti, G., Chamberlain, J.S., Wright, W.E., Torrente, Y., Ferrari, S., Bianco, P., Cossu, G., 2007. Pericytes of human skeletal muscle are myogenic precursors distinct from satellite cells. *Nat. Cell Biol.* 9, 255–267.
- Deng, S., Azevedo, M., Baylies, M., 2017. Acting on identity: Myoblast fusion and the formation of the syncytial muscle fiber. *Semin. Cell Dev. Biol.* 72, 45–55.
- Diaz-Flores, L., Gutierrez, R., Madrid, J.F., Varela, H., Valladares, F., Acosta, E., Martin-Vasallo, P., Diaz-Flores Jr., L., 2009. Pericytes. Morphofunction, interactions and pathology in a quiescent and activated mesenchymal cell niche. *Histol. Histopathol.* 24, 909–969.
- Diaz-Manera, J., Touvier, T., Dellavalle, A., Tonlorenzi, R., Tedesco, F.S., Messina, G., Meregalli, M., Navarro, C., Perani, L., Bonfanti, C., Illa, I., Torrente, Y., Cossu, G., 2010. Partial dysferlin reconstitution by adult murine mesoangioblasts is sufficient for full functional recovery in a murine model of dysferlinopathy. *Cell Death Dis.* 1, e61.
- Goritz, C., Dias, D.O., Tomilin, N., Barbacid, M., Shupliakov, O., Frisen, J., 2011. A pericyte origin of spinal cord scar tissue. *Science* 333, 238–242.
- Guimaraes-Camboa, N., Cattaneo, P., Sun, Y., Moore-Morris, T., Gu, Y., Dalton, N.D., Rockenstein, E., Masliah, E., Peterson, K.L., Stallcup, W.B., Chen, J., Evans, S.M., 2017. Pericytes of multiple organs do not behave as mesenchymal stem cells in vivo. *Cell Stem Cell* 20 (345–359), e345.
- Hayashiji, N., Yuasa, S., Miyagoe-Suzuki, Y., Hara, M., Ito, N., Hashimoto, H., Kusumoto, D., Seki, T., Tohyama, S., Kodaira, M., Kunitomi, A., Kashimura, S., Takei, M., Saito, Y., Okata, S., Egashira, T., Endo, J., Sasaoka, T., Takeda, S., Fukuda, K., 2015. G-CSF supports long-term muscle regeneration in mouse models of muscular dystrophy. *Nat. Commun.* 6, 6745.
- Joe, A.W., Yi, L., Natarajan, A., Le Grand, F., So, L., Wang, J., Rudnicki, M.A., Rossi, F.M., 2010. Muscle injury activates resident fibro/adipogenic progenitors that facilitate myogenesis. *Nat. Cell Biol.* 12, 153–163.
- Kabara, M., Kawabe, J., Matsuki, M., Hira, Y., Minoshima, A., Shimamura, K., Yamauchi, A., Aonuma, T., Nishimura, M., Saito, Y., Takehara, N., Hasebe, N., 2014. Immortalized multipotent pericytes derived from the vasa vasorum in the injured vasculature. A cellular tool for studies of vascular remodeling and regeneration. *Lab. Invest.* 94, 1340–1354.
- Khan, J.A., Mendelson, A., Kunisaki, Y., Birbrair, A., Kou, Y., Arnal-Estape, A., Pinho, S., Ciero, P., Nakahara, F., Ma'ayan, A., Bergman, A., Merad, M., Frenette, P.S., 2016. Fetal liver hematopoietic stem cell niches associate with portal vessels. *Science* 351, 176–180.
- Klimczak, A., Kozłowska, U., Kurpisz, M., 2018. Muscle stem/progenitor cells and mesenchymal stem cells of bone marrow origin for skeletal muscle regeneration in muscular dystrophies. *Arch. Immunol. Ther. Exp. (Warsz)* 66, 341–354.
- Kramann, R., Schneider, R.K., DiRocco, D.P., Machado, F., Fleig, S., Bondzie, P.A., Henderson, J.M., Ebert, B.L., Humphreys, B.D., 2015. Perivascular Gli1+ progenitors are key contributors to injury-induced organ fibrosis. *Cell Stem Cell* 16, 51–66.
- Mendelson, A., Frenette, P.S., 2014. Hematopoietic stem cell niche maintenance during homeostasis and regeneration. *Nat. Med.* 20, 833–846.
- Minasi, M.G., Riminucci, M., De Angelis, L., Borello, U., Berarducci, B., Innocenzi, A., Caprioli, A., Sirabella, D., Baiocchi, M., De Maria, R., Boratto, R., Jaffredo, T., Broccoli, V., Bianco, P., Cossu, G., 2002. The meso-angioblast: a multipotent, self-renewing cell that originates from the dorsal aorta and differentiates into most mesodermal tissues. *Development* 129, 2773–2783.
- Minoshima, A., Kabara, M., Matsuki, M., Yoshida, Y., Kano, K., Tomita, Y., Hayasaka, T., Horiuchi, K., Saito, Y., Aonuma, T., Nishimura, M., Maruyama, K., Nakagawa, N., Sawada, J., Takehara, N., Hasebe, N., Kawabe, J.I., 2018. Pericyte-specific *ninjurin1* deletion attenuates vessel maturation and blood flow recovery in hind limb ischemia. *Arterioscler. Thromb. Vasc. Biol.* 38, 2358–2370.
- Mitchell, K.J., Pannerec, A., Cadot, B., Parlakian, A., Besson, V., Gomes, E.R., Marazzi, G., Sassoon, D.A., 2010. Identification and characterization of a non-satellite cell muscle resident progenitor during postnatal development. *Nat. Cell Biol.* 12, 257–266.
- Morrison, S.J., Scadden, D.T., 2014. The bone marrow niche for haematopoietic stem cells. *Nature* 505, 327–334.
- Phinney, D.G., Prockop, D.J., 2007. Concise review: mesenchymal stem/multipotent stromal cells: the state of transdifferentiation and modes of tissue repair—current views. *Stem Cells* 25, 2896–2902.
- Rodriguez, A.M., Pisani, D., Dechesne, C.A., Turc-Carel, C., Kurzenne, J.Y., Wdziekonski, B., Villageois, A., Bagnis, C., Breittmayer, J.P., Groux, H., Ailhaud, G., Dani, C., 2005. Transplantation of a multipotent cell population from human adipose tissue induces dystrophin expression in the immunocompetent *mdx* mouse. *J. Exp. Med.* 201, 1397–1405.
- Shi, X., Garry, D.J., 2006. Muscle stem cells in development, regeneration, and disease. *Genes Dev.* 20, 1692–1708.
- Susaki, E.A., Tainaka, K., Perrin, D., Kishino, F., Tawara, T., Watanabe, T.M., Yokoyama, C., Onoe, H., Eguchi, M., Yamaguchi, S., Abe, T., Kiyonari, H., Shimizu, Y., Miyawaki, A., Yokota, H., Ueda, H.R., 2014. Whole-brain imaging with single-cell resolution using chemical cocktails and computational analysis. *Cell* 157, 726–739.
- Tomita, Y., Horiuchi, K., Kano, K., Tatsukawa, T., Matsuo, R., Hayasaka, T., Yoshida, Y., Kabara, M., Yasuda, S., Nakajima, K., Nakagawa, N., Takehara, N., Okizaki, A., Hasebe, N., Kawabe, J.I., 2019. *Ninjurin 1* mediates peripheral nerve regeneration through Schwann cell maturation of NG2-positive cells. *Biochem. Biophys. Res. Commun.*
- Yamauchi, A., Kawabe, J., Kabara, M., Matsuki, M., Asanome, A., Aonuma, T., Ohta, H., Takehara, N., Kitagawa, T., Hasebe, N., 2013. *Apurinic/aprimidinic endonuclease 1* maintains adhesion of endothelial progenitor cells and reduces neointima formation. *Am J Physiol Heart Circ Physiol* 305, H1158–H1167.
- Yin, H., Price, F., Rudnicki, M.A., 2013. Satellite cells and the muscle stem cell niche. *Physiol. Rev.* 93, 23–67.
- Yoshida, Y., Kabara, M., Kano, K., Horiuchi, K., Hayasaka, T., Tomita, Y., Takehara, N., Minoshima, A., Aonuma, T., Maruyama, K., Nakagawa, N., Azuma, N., Hasebe, N., Kawabe, J.I., 2020. Capillary-resident EphA7(+) pericytes are multipotent cells with anti-ischemic effects through capillary formation. *Stem Cells Transl Med* 9, 120–130.
- Zhao, H., Feng, J., Seidel, K., Shi, S., Klein, O., Sharpe, P., Chai, Y., 2014. Secretion of *shh* by a neurovascular bundle niche supports mesenchymal stem cell homeostasis in the adult mouse incisor. *Cell Stem Cell* 14, 160–173.